

# Research on a novel compact linac<sup>\*</sup>

LUO Xiao-Wei(罗小为)<sup>1,2;1)</sup> XIANG Xin-Lei(相新蕾)<sup>2;2)</sup> XIE Jia-Lin(谢家麟)<sup>2)</sup>

<sup>1</sup> Institute of Nuclear Technology, University of Science and Technology of China, Hefei 230027, China

<sup>2</sup> Institute of High Energy Physics, Chinese Academy of Sciences, Beijing 100049, China

**Abstract:** This work looks at a new type of electron linear accelerator. Compared with the traditional electron linac, it has only two main parts: a klystron and an accelerating tube, without the electron gun element. This new kind of linac could perform just like its predecessors but reduce cost and space. The preliminary design and simulation have been accomplished. In this paper, an overview discussion about the performance tests and some improvements to increase the beam current are presented.

**Key words:** klystron, ending beam, linac, bunched injector

**PACS:** 29.17.+w, 29.25.Bx      **DOI:** 10.1088/1674-1137/35/1/020

## 1 Introduction

The electron linac is a widely used device in industrial, electronic, medical and scientific research fields. The traditional linac consists of three main parts: a microwave power source, an electron source and an accelerating structure. A high power klystron has long been adopted for microwave supplies, while the spent beam is absorbed by the collector. A series of studies with these spent electrons has been carried out and the results indicate phase clustering of a small part of the higher energy electrons. Thus, a program using a magnetic field to select the spent electrons with suitable energy and phase to inject into an accelerator section is conducted. This made the high energy klystron not only the microwave power source but also the electron source, while many components of conventional linacs can be omitted to simplify construction and maintenance and to reduce costs.

After taking every possible factor into consideration [1], we decided to make a Proof-of-Principle structure with a 5 MW klystron.

## 2 Structure

In the klystron, a bunched electron beam generates microwave power at the output cavity while some

unbunched electrons are accelerated by the microwave field of the output cavity. Part of the spent beam will pass through a hole at the top of the collector of the klystron and enter the bending magnetic field region. A set of adjustable slits working as a collimator is located at the exit of the magnet field that can allow a chosen portion of the beam to be injected into an achromatic beam transport system to accommodate different output beam directions for acceleration or other applications. Fig. 1 shows the main components of the structure.

Because of financial constraints, we have chosen the KS4064 klystron as the power source and electron source. Table 1 shows the klystron operating parameters.

The Arsenal-MSU program is used to simulate the electron motion in a KS4064 klystron (5 MW) under the typical operation conditions of 126 kV and 89 A. This is a 2.5 D code tracing the coordinates  $r$ ,  $z$ , and the momentum  $P_z$ ,  $P_r$ ,  $P_c$  of the macro-electrons along the drift space. The simulation was carried out up to the top of the collector to allow the passage of the spent beam through a short drift tube which serves as an emittance filter as well as a current limiter. Fig. 2 shows the energy versus current distributions of the macro-electrons at the entrance of the bending magnet.

---

Received 28 April 2010

\* Supported by National Natural Science Foundation of China (10555001)

1) E-mail: zhanny@ustc.edu

2) E-mail: xiangxl@ihep.ac.cn

©2011 Chinese Physical Society and the Institute of High Energy Physics of the Chinese Academy of Sciences and the Institute of Modern Physics of the Chinese Academy of Sciences and IOP Publishing Ltd

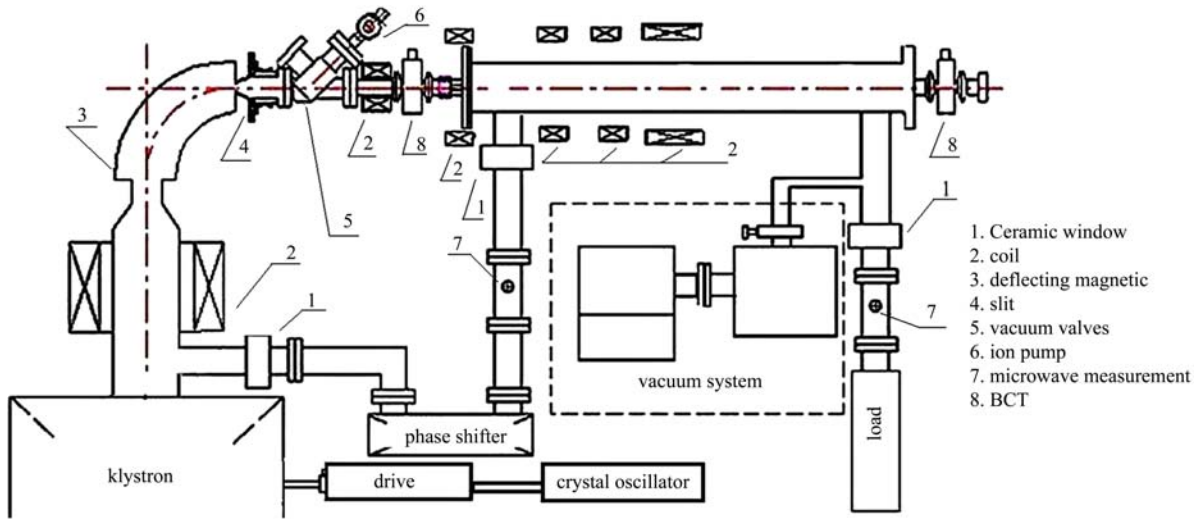


Fig. 1. Main components of the linac.

Table 1. The KS4064 klystron operating parameters.

	design value [2]	measured value
peak beam voltage	127 kV	126 kV
peak beam current	90 A	89 A
pulse duration	5.8 $\mu$ s	6.0 $\mu$ s
heater current	7.5 V	7.5 V
vacuum	$< 1.33 \times 10^{-4}$ Pa	$< 10^{-6}$ Pa
vacuum pump voltage	3 kV	3 kV
peak driver power	150 W	143 W
peak output power	5.5 MW	5.1 MW
pulse repeat ratio	180	

to get high energy [3]. Table 2 shows the accelerating tube parameters.

Table 2. Accelerating tube parameters.

operating mode	traveling wave
frequency	2857 MHz
mode	$2\pi/3$
shunt impedance	63 M $\Omega$ /m
VSWR	1.02
$Q$ factor	13700
attenuation factor	4.1 dB
total length	1.39 m

The phase shift between the cavities in the accelerating tube is about  $\pm 1^\circ$ . The following formula shows the energy change caused by the phase shift [4],

$$\frac{\delta U}{U} = \frac{N\Theta_q^2}{4} \left[ 2 + \frac{2}{\tau} + \frac{2}{e^{-\tau} - 1} \right] + \frac{N\Theta_q^2}{12} \left[ \frac{6}{\tau \tanh \frac{\tau}{2}} - \frac{12}{\tau^2} \right],$$

where  $\Theta_q$  [rad] stands for the single cavity phase shift error between the cavities,  $N$  for the number of cavities,  $U$  for the electron energy and  $\tau$  [Nb] for the attenuation constant. Based on the above test results,

$$\frac{\delta U}{U} = 0.8\%.$$

Filling time

$$t_F = \frac{2Q\tau}{\omega},$$

where design  $Q = 13700$ ,  $\tau = 0.41$  Nb,  $\omega = 2\pi f$  ( $f = 2856$  MHz).  $t_F$  was calculated as 626.0 ns compared with the measured value 690.5 ns.

### 3 Experiments and results

Two BCTs were set before and after the accelerating tube for beam measurement. At the end of

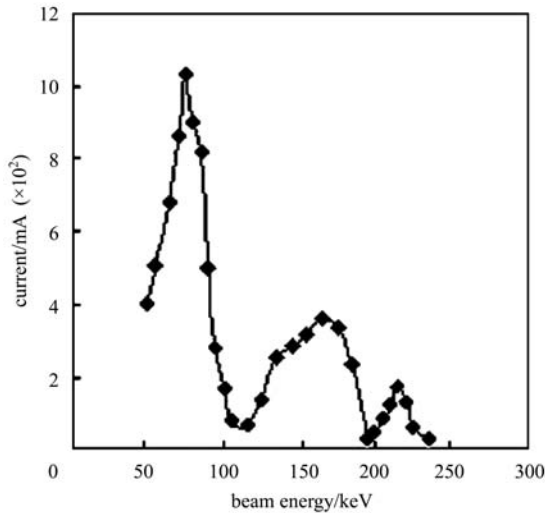


Fig. 2. Energy of macro-electrons at the entrance of the bending magnetic field vs beam intensity.

After the extraction system electrons of 170 keV and 210 keV were obtained, these cluster electrons had a phase width of less than  $30^\circ$  and were injected into an accelerating structure consisting of 38 constant impedance cells plus input and output couplers

the structure, a Faraday cage was used to collect the accelerated beam. The working repetition rate is 12.5 Hz and the high voltage is 126 kV.

The beam capture rate is different due to the change in the high frequency microwave power phase with the widths of the optical grating at 8 mm. The maximum beam intensity is 102 mA with the beam injected at 170 keV. Fig. 3(a) shows the input and output beam intensity measured by BCT. Fig. 3(b) shows the pulse measured by the Faraday cage. Due to the filling time in the accelerator (measured experimentally), the output spectra width of the Faraday cage is about 0.8  $\mu$ s narrower than that of the microwave power. 170 keV injected beam capture is about 72% compared with 81% of the 210 keV injected beam.

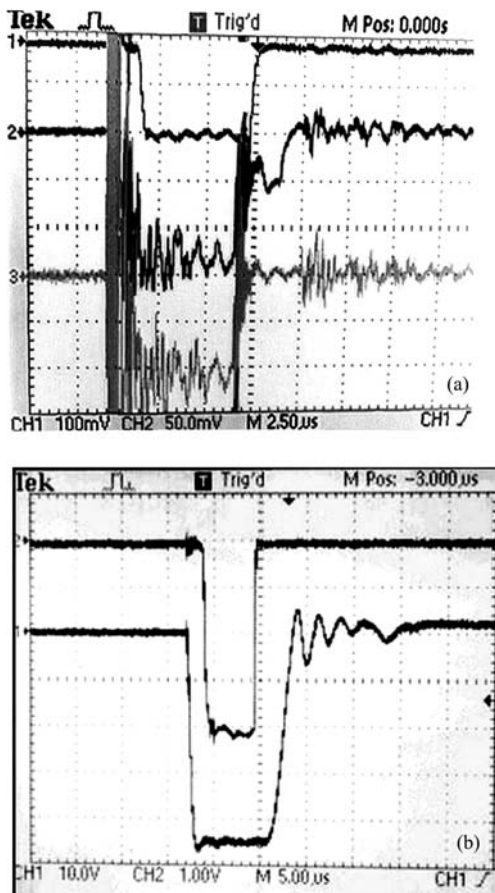


Fig. 3. (a) Pulse measurement (CH1 for the microwave power; CH2 for the input beam intensity, 139 mA; CH3 for the output beam intensity, 104 mA). (b) Pulse measurement (CH1 for the Faraday cage, 101 mA; CH2 for the pulsed high voltage).

To measure the size of the output beam, the target was placed at the exit of the accelerator (after the 75  $\mu$ m thick output aluminum window). Fig. 4 shows the beam spot under different conditions. The

S-curve of the shadow gray value and charge density was obtained from the experiment. The resultant beam size shows that 90 percent particles within an area with 4 mm in radius.

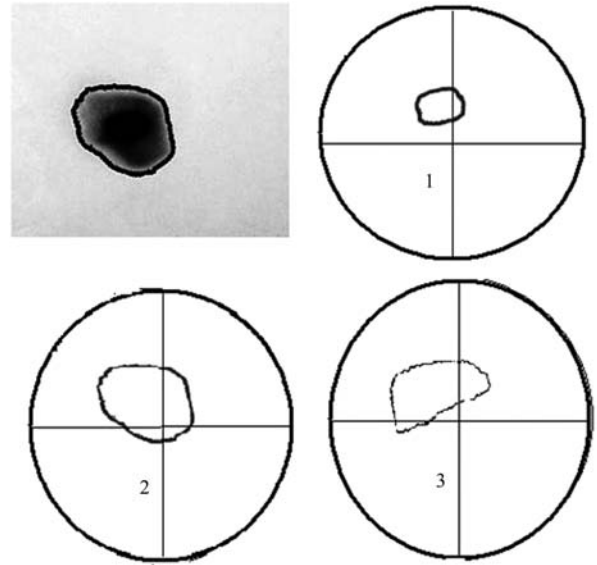


Fig. 4. The target measured beam spot under different conditions (Item 1 for the 210 keV beam output at 28 mA, item 2 for the 170 keV beam output at 104 mA, item 3 for the 170 keV beam output at 80 mA. The outside circle is the 12.5 mm radius aluminum window.).

In the measurement program of the accelerated beam energy, the collimator and the beam absorber are made of 2.5 cm thick lead with the purpose of absorbing the 10 MeV-level escaping electrons from the track centre. The slit width is about 2 mm at the collimator and beam absorber. The analysis magnet

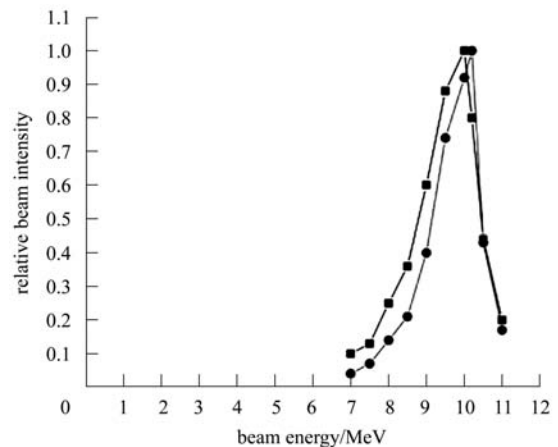


Fig. 5. Energy spectra (The narrow one is for the 210 keV beam output at 28 mA, and the wide one is for the 170 keV beam output at 80 mA).

is working at a centre track radius of 125 mm and deflection angle of  $45^\circ$ . Through the adjustment of the analysis magnet current, a signal is achieved by the ionization chamber and the Faraday cage. Fig. 5 shows the energy spectrum. It shows that 10 MeV level electrons will be obtained by the structure as expected. The FWHM spectrum broadening is within 14% to 9% under different injected beam energies.

## 4 Discussion

More research will be conducted to improve the performance of devices. Parmela code shows that the optimization of the device to reduce the 170 keV injected beam loss at the vacuum valves and drift tube may let the beam intensity increase to 140 mA, which is more suitable for industrial use of irradi-

ation. 210 keV injected beam with lower beam intensity provides a good beam performance for the experimental work. This plan shows its advantages in higher energy linacs, for example, for a 30 MeV linac. Parmela code shows that the spending beam of a 30 MW klystron at 400 keV, 300 mA will be accelerated with the beam capture above 95% and the FWHM spectrum broadening less than 7%. In this case, additional focus is no longer required.

In conclusion, it is the first time that the properties of the 5 MW klystron have been measured. The experiment provides direct evidence that it is feasible to use this kind of spending beam as the injecting beam of E-LINAC. Furthermore, since the spending beam from a klystron is bunched, a lot of apparatuses like bunchers can be omitted. The program shows an economical and simple way for further study.

---

## References

- 1 XIE Jia-Lin, WANG Fa-Ya et al. RSI, 2003, **12**: 5053–5057
- 2 SHEN Bin. KS4064-5 MW Klystron Performance: The Institute of Electronics. Chinese Academy of Sciences, 2002.8
- 3 WANG Fa-Ya. HEP & NP, 2004, **10**: 105–109 (in Chinese)
- 4 Lapostolle, Pierre M. Linear Accelerators. Amsterdam: North Holland Pub. Co., 1970. 55